



Electrochemical conversion of pressurized CO₂ at simple silver-based cathodes in undivided cells: study of the effect of pressure and other operative parameters

Federica Proietto¹ · François Berche¹ · Alessandro Galia¹ · Onofrio Scialdone¹

Received: 6 July 2020 / Accepted: 9 November 2020 / Published online: 27 November 2020
© The Author(s) 2020

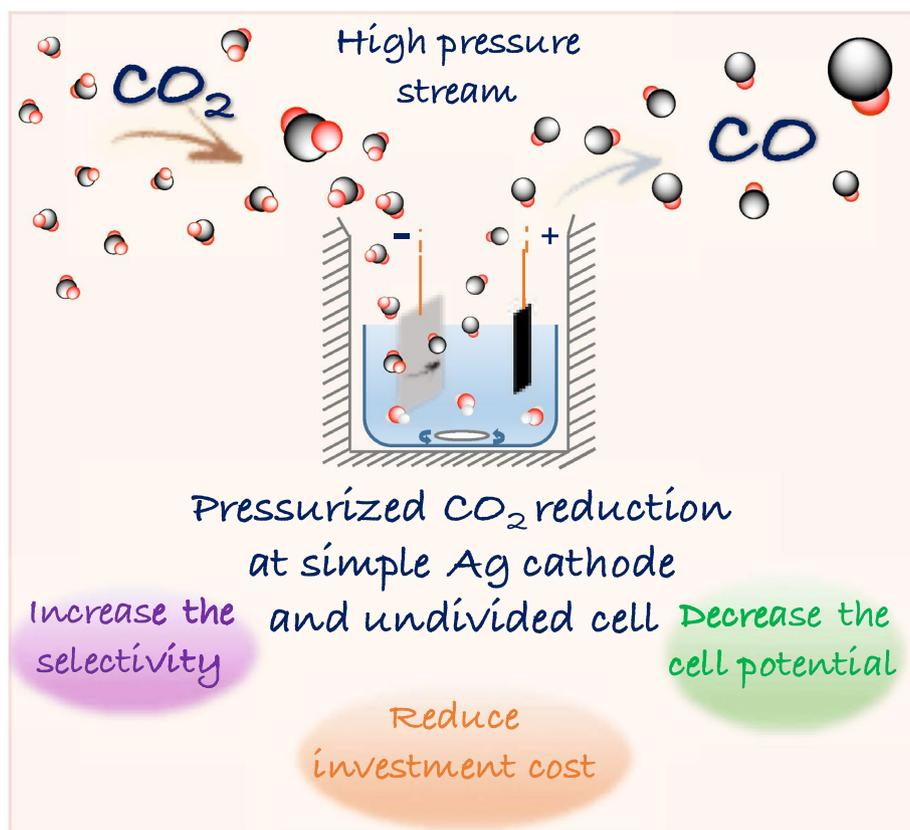
Abstract

Electrochemical reduction of pressurized CO₂ is proposed as an interesting approach to overcome the main hurdle of the CO₂ electrochemical conversion in aqueous solution, its low solubility (ca. 0.033 M), and to achieve good faradaic efficiency in CO using simple sheet silver cathodes and undivided cells, thus lowering the overall costs of the process. The effect on the process of CO₂ pressure (1–30 bar), current density, nature of the supporting electrolyte and other operative conditions, such as the surface of the cathode or the mixing rate, was studied to enhance the production of CO. It was shown that pressurized conditions allow to improve drastically the current efficiency of CO (CE_{CO}). Furthermore, at relatively high pressure (20 bars), the utilization of simple sheet silver cathodes and silver electrodes with high surfaces gave similar CE_{CO}. The stability of the system was monitored for 10 h; it was shown that at a relatively high pressure (15 bar) in aqueous electrolyte of KOH using a simple plate silver cathode a constant current efficiency of CO close to 70% was obtained.

✉ Onofrio Scialdone
onofrio.scialdone@unipa.it

¹ Dipartimento di Ingegneria Università degli Studi di Palermo, Viale delle Scienze, Ed. 6, 90128 Palermo, Italy

Graphic abstract



Keywords CO_2 · Carbon monoxide · Pressure · Reduction · Silver

1 Introduction

Nowadays, in a world struggling to curb the global warming, electrochemical conversion of carbon dioxide could be considered one of the main strategies for both synthesis of chemicals and decrease of CO_2 emissions [1–3]. Recently, Bushuyev et al. [4] have discussed the current state of emerging technologies for the catalytic conversion of carbon dioxide into various chemical products, keeping in consideration the economics of the process. They visualized at least six potentially disruptive CO_2 catalytic conversion technologies (i.e. electrocatalysis, photocatalysis, biohybrid, nanoporous confinement, etc.), envisioning a timeline for their implementation on a large scale and reaching the conclusion that the closest technologies to commercialisation with start-up and entrenched companies (i.e. Opus-12, Dioxide Material, and Carbon Recycling International) are based on CO_2 electrochemical conversion. More in general, the Carbon Capture and Utilization (CCU) technologies become more attractive as the renewable energy price continues to decline (getting to 2 ¢/kWh in some jurisdictions) and the process

could utilize the excess electric energy from intermittent renewable sources to transform CO_2 into carbon-based chemicals, storing electric energy in the form of chemical energy [2, 4, 5]. Electrochemical conversion of CO_2 is challenging because of (i) low stability, (ii) high overpotential, (iii) low solubility of CO_2 in aqueous electrolytes at ambient conditions (ca. 34 mM), (iv) in some cases high catalyst cost, and (v) low productivity often associated to high products selectivity [6, 7]. To date, among the wide range of chemical products produced by the CO_2 electrochemical reduction in water solvent [8–14], the highest current efficiencies (CEs) and current densities (j) are usually reported for CO and formate/formic acid ($2e^-$ reduction products) [3, 6]. Furthermore, some studies have shown that CO, formic acid and other carboxylic acids can be produced in aprotic solvents by CO_2 reduction [15, 16]. In aqueous electrolytes, several catalysts are known to selectively lead to the production of CO (i.e. Ag, Zn, Au, Cu) [17]; in particular, Ag and Au based electrodes allow to achieve quite high CE in CO (CE_{CO}) in short electrolyses and they are characterized by relatively low overpotential values for the hydrogen

evolution reaction (HER) allowing to obtain both CO and H₂. Among the noble metals, the Ag electrode is considered one of the more promising materials for the scale-up of the CO₂ reduction process due to its lower market cost with respect to Au and good faradic efficiency [18].

While, at the beginning, the formation of CO from CO₂ reduction was investigated using conventional plate electrodes [17], in last years, many researchers have focused their attention on the engineering of better electrodes, catalyst, electrolyte composition and configuration of electrolyser [6, 19, 20] to improve the performances of the process. In particular, attention was devoted on overcoming one of the main issues of the electrochemical conversion of CO₂ in water solution: its low concentration, resulting in low CO₂ conversion rate (limited by mass transport limitations) and in low productivity or/and low current efficiencies.

Several works have shown that the implementation of electrodes with high active surface allows operating at higher current intensities than that achieved at simple plate electrodes improving the performances of the process [21–27]. For example, Lu [23] and Ma [22] and co-workers have synthesized, respectively, a nanoporous (np-Ag) and an oxide-derived nanostructured (OD-Ag) silver catalyst (i.e. both structures characterized by a larger area for catalytic reaction than that of polycrystalline silver) which allow, at low overpotentials, to achieve a *j* at least 20 times higher than that reached at planar Ag and increase drastically the CE_{CO} from less than 4% using a plate silver to 80 or 92% using OD-Ag or np-Ag electrode, respectively, in a CO₂ saturated aqueous KHCO₃ electrolyte. Electrodes with high active surface for low overpotentials are characterized by a lower value of the Tafel slope (i.e. 58 and 77 mV dec⁻¹ for np-Ag and OD-Ag, respectively) than the polycrystalline silver electrode (~130 mV dec⁻¹), that indicates a fast initial electron transfer to a CO₂ molecule speeding up the reduction rate; however, at relatively high overpotentials, the Tafel slope increases, thus showing that, also for this kind of electrodes, the CO₂ electrochemical conversion could be limited by the mass transport of CO₂ to the surface of the electrode [6, 22, 23, 28].

Another strategy to reduce mass transfer limitations due to the low concentration of CO₂ dissolved in aqueous electrolyte at atmospheric pressure is the utilization of gas diffusion electrodes (GDEs), that make faster the reactant transport and distribution [3, 13, 29–31]. Ma et al. [24] have shown that it is possible to achieve a nominal current density up to 350 mA cm⁻² with high faradic efficiency (CE_{CO} ~ 95%) and an energy efficiency of CO (EE_{CO}) of about 45% working with an Ag-GDE at 3 V in alkaline media (1 M KOH) for a short time. In addition, under adopted conditions, the utilization of a Ag-GDE can guarantee a quite high conversion ratio up to 32% per pass maintaining a CE_{CO} close to 80% [32]. To date, although the implementation of GDEs

gave very promising results in term of CE_{CO, j} and productivity [3, 11, 33, 34], there are some challenges that should be solved. Most of the GDEs are suffering from (i) loss of the catalyst possibly due to the low adhesion of the common-used Nafion solution as a binder of the catalyst to the support; (ii) low stability with the time; (iii) high overall costs; and, (iv) salt deposition on the gas diffusion layer determining blocking of CO₂ access in the GDE [35, 36]. Furthermore, a crucial factor, using a GDE-type cell, is the pressure balance between the gas and liquid compartments to avoid that the gas can go through the gas diffusion layer, not allowing the essential three-phases contact (among the solid catalyst, liquid electrolyte and gas reagent), or flooding of the gas compartment due to the electrolyte.

To enhance CO₂ solubility and its reduction rate to added value products, other researchers are focusing their attention on the utilization of pressurized CO₂ in aqueous electrolyte [37–48] or in ionic liquid-based electrolytes (ILs) [49–55]. Indeed, according to several authors, the pressure can affect the selectivity between CO₂ and water reduction, the distribution of the CO₂ reduction products and overpotentials need to drive the reaction [37–46]. In particular, a dramatic effect of pressure on electrochemical conversion of CO₂ to formic acid in aqueous electrolyte at tin cathodes was observed by some authors [42, 44, 56–58]. Moreover, among the limited number of studies employing high pressure for the CO₂ reduction, Pardal et al. [54] have showed that the combination of high CO₂ pressure with ionic liquid-based electrolyte, as CO₂ adsorption media, can significantly improve the productivity of the process by maintaining high selectivity of the process towards CO (CO productivity of about 0.25 mmol cm⁻² coupled with a CE_{CO} ~ 97% after a passed charge of about 50 °C at 30 bar, 45 °C and – 0.8 V vs RHE).

First data about high pressure CO₂ electrochemical conversion at silver cathodes in water electrolyte were reported by Hara et al. [37] in 1995, showing that it is possible to obtain a quite high CE_{CO} (~ 75%) at 30 bar using an Ag plate electrode in a divided cell equipped with a Nafion 117. In spite of these very promising results, few studies were devoted later on the potential utilization of pressurized CO₂ for its electrochemical conversion to CO mainly using a GDE with a promising result for short electrolysis. In particular, Dufek and co-workers [41, 45] have shown an improvement in CE_{CO} (~ 80%) and in reduction rate (~ 220 mA cm⁻²) with a corresponding suppression of hydrogen evolution reaction by working in K₂SO₄ aqueous electrolyte at an elevated pressure of about 20 bar for 1 h. More recently, it has been demonstrated by Gabardo et al. [46] that an increase in the performances of the process can be achieved due to the synergetic effect of very highly alkaline reaction environment (1–7 M KOH aqueous electrolyte), which decreases the overpotentials (thus enhancing the

energetic efficiency), and pressurized CO₂ system (up to 7 bars), which inhibits the production of other CO₂ reduction products (thus increasing the selectivity). Conversely, other studies have shown that the utilization of the pressure change remarkably the CO₂ product distribution; for example, Hara [38] found that an enhancement of the CO₂ pressure and/or mixing rate at Cu-based electrodes can selectively drive the electrochemical reduction to CO, HCOOH, H₂ or hydrocarbons. However, due to the problems and costs of GDEs based electrodes, it would be interesting to focus on the utilization of simpler cathodes under pressurized conditions. In particular, we would like to focus on the possibility to use pressurized carbon dioxide to convert it effectively to CO using relatively simple and cheap apparatuses such as undivided cells (in order to avoid the economic penalties given by the separator) and simple plate silver cathodes (in order to avoid the costs connected with more complex electrodes) by studying the effect of different operative parameters. In this frame, it is important to remind that (i) the utilization of not too high pressures involves a quite low operative and capital costs [59] (ii) pressurized condition could aid the industrial integration of the CO₂ reduction process with up- and downstream processes and, (iii) in spite the wide literature on the CO₂ reduction to CO, up to our knowledge, no other studies are focused on the investigation of several operative parameters under pressurized conditions at flat Ag on the performances of the process. Hence, in this work the electrochemical conversion of CO₂ to CO was studied at simple silver electrodes with the aim to better evaluate the effect of the pressure (1–30 bar) and of various operative conditions (current density, nature of the supporting electrolyte, surface of the electrode, etc.) under pressurized conditions on the performances of the process. As previously mentioned, the utilization of electrodes with high active surface for CO₂ reduction could be an interesting alternative to improve the performances of the process; hence, the synergetic utilization of a cathode with high surface and pressurized CO₂ was also studied, comparing the results with that achieved with a silver plate cathode. Eventually, it was studied the stability of the CO production at relatively high pressure (15 bars) using different electrolytes for 10 h.

2 Materials and experimental methods

2.1 Reagents, materials and analyses

An electrolytic solution composed of bi-distilled water as solvent and 0.2 M K₂SO₄ (purity > 99.0%, Janssen Chimica), 0.5 M KOH (purity > 86.7%, VWR Chemicals), 0.5 M KHCO₃ (purity > 99.7%, Aldrich) or 0.5 M KCl (purity > 99.5%, Fluka) as supporting electrolyte has been employed. The solution pH was measured with a Checker®

pH Tester (HI98103) supplied by HANNA® instruments. To feed the system, CO₂ (99.999% purity) supplied from Rivoir was employed. Silver plate (plate-Ag) and a high surface silver electrode (hs-Ag) based on commercial nanoparticles supported on carbon fiber paper (PTFE treated to 5%) were used as working electrode. The hs-Ag electrodes were prepared via hand-painting techniques according the procedure described in [60]; the catalyst ink was prepared by mixing Ag catalyst (unsupported Ag nanoparticles, < 100 nm particle size, 99.5% trace metals basis, Sigma-Aldrich), deionized H₂O (200 µL), Nafion® perfluorinated resin solution (5 wt% in lower aliphatic alcohols and water, $\rho = 0.874$ g/mL, Sigma Aldrich; 10:1 catalyst-to-Nafion ratio) and isopropyl alcohol (200 µL). Subsequently, the ink was sonicated for 20 min by a LabSonic FalcSonicator, hand-painted using a paintbrush to cover with catalyst a total geometrical area of 1.5 cm² and dried under an atmosphere of N₂ (99.999% purity; supplied by Air Liquide). The actual catalyst loading was of 0.5 mg cm⁻². Agilent HP 1100 HPLC fitted with Rezex ROA-Organic Acid H⁺ (8%) column (Phenomenex) at 55 °C and coupled with a UV detector working at 210 nm was used to evaluate the formic acid concentration. The used mobile phase is a 0.005 N H₂SO₄ water solution at pH 2.5 eluted at 0.6 mL min⁻¹. To calibrate the HPLC instrument, a pure standard of HCOOH (99–100%, supplied by Sigma-Aldrich) was used. Gas chromatography analyses were made to characterize the gas products compositions (H₂, CO, CO₂, O₂, N₂ and CH₄). A gas-tight syringe (supplied by Hamilton GASTIGHT®) was used to take a gas sample of 250 µL from a pierceable septum located in the effluent gas stream. Agilent 7890B GC equipped with a Carboxen-1000 (60/80) column and a Thermal Conductivity Detector (at 230 °C) was used. Helium (Air Liquide 99.999% purity) was used as carrier gas with constant pressure set at 1 bar; the column temperature program was an isotherm at 35 °C for 5 min followed by a 20 °C min⁻¹ ramp up to 225 °C and by an isothermal step for 45 min.

2.2 Electrochemical characterization

Linear sweep voltammetry (LSV) characterizations were carried out using: (i) a conventional three-electrode cell with a SCE reference (Radiometer analytical) and a Pt wire counter electrode (system I); and (ii) cylindrical AISI 316 stainless steel cell able to work at high CO₂ pressure (system II), described in detail in previous work [44]. The latter was utilized to perform pseudo-polarization curves at relatively high pressure of CO₂ (range 1–30 bar) as a function of the overall cell potential. The geometric area of the working electrode was 0.1 cm². Stirring of the solution was made with a magnetic stirrer. Characterizations were performed at 0 and 500 rpm. Prior to all characterization, the solution was purged for 25 min by either N₂ (99.999% purity; supplied by

Air Liquide) or CO₂ (99.999% purity; supplied by Rivoira). LSVs were performed under N₂ and CO₂ atmosphere with a scan rate of 0.005 V s⁻¹ using an AutoLab PG-STAT12. The $j_{\text{CO}_2\text{-N}_2}$ was calculated under the assumption that the current of the H₂ evolution and CO₂ reduction can add up and H₂O reduction is the only competitive reaction to the CO₂ conversion at the cathode surface.

2.3 Electrolysis

Electrolysis were carried out using two different systems. System I was a conventional batch undivided glass cell equipped with a gas inlet, plate-Ag (3 cm²) or hs-Ag (1.5 cm²) as cathode, a compact graphite (from Carbon Lorraine) or a Ti/IrO₂-Ta₂O₅ sheet anode (from ElectroCell AB) as anode and a SCE reference electrode (Radiometer analytical). System II was an undivided cylindrical AISI 316 stainless steel cell able to work at high pressure of CO₂, described in detail in previously work [44]. Briefly, it was equipped with a gas inlet, a pressure gauge, a dip tube connected to a pressure relief valve and two electrical line connections for the electrodes. The system worked with a continuous supply of carbon dioxide without accumulation of gases. CO₂ was used to pressurize the system at a flow of about 100 mL min⁻¹ and the operative pressure was controlled using a pressure reducer. Stirring of the solution ($V=0.05$ L) was performed with a magnetic stirrer. The electrode gap was about 1 cm for both systems. Before each electrolyses, plate-Ag electrode was firstly polished with an alumina powder suspension (size 1 μm), sonicated in bi-distillate water for 10 min, and then rinsed with bi-distillate water. Compact graphite was mechanically scrubbed with sandpaper (P-800) and sonicated in bi-distillate water until the water resulted in transparently. The DSA® anode was polished by ultrasound bath in bi-distillate water. The current density was calculated as the ratio between the current intensity and the wet surface area of the cathode exposed to the anode. Electrolyses were performed under galvanostatic condition (Amel 2053 potentiostat/galvanostat) at room temperature. Experiments were repeated at least twice with a reproducibility within 6% of the results. The instantaneous current efficiency (CE), energetic efficiency (EE) and the energetic consumption (Wh/mol_{CO}) were defined, as follows:

$$CE_i = 2Fn_i/It;$$

$$EE = E_{\text{cell}}^{\circ} CE_{\text{CO}}/\Delta V;$$

$$\text{Energetic consumption} = I * \Delta V/n_{\text{CO}}$$

where F is the faradaic constant (96,485 C mol⁻¹), n_i mole of i product and I the current intensity, t the time, E_{cell}° is the standard cell potential: -1.33V for the electroreduction

for CO₂ to CO coupled to O₂ evolution, ΔV the applied cell potential.

The CO production rate, r_{CO} , (mol h⁻¹ m⁻²) was calculated as follow:

$$r_{\text{CO}} = CE_{\text{CO}}j/2F,$$

where the CE_{CO} is the current efficiency of CO, j the current density (A m⁻²).

The limiting current density $j_{\text{lim}} = zF(D/\delta)c^b\text{CO}_2$ (where z is the number of electrons involved in the CO₂ reduction, F the faraday constant (96,485 C mol⁻¹), D the CO₂ diffusion coefficient, δ the thickness of the stagnant layer and $c^b\text{CO}_2$ the bulk CO₂ concentration) was computed considering the solubility of CO₂ in water, $c^b\text{CO}_2$, at 25 °C [61], $D = 1.94 \cdot 10^{-9}$ m² s⁻¹ [42] while δ was previously estimated in our laboratory [62] for each adopted mixing rate through a well-known diffusion limiting current technique using a very stable redox couple Fe(II)/Fe(III).

3 Results and discussion

3.1 Electrochemical conversion of carbon dioxide to CO at various pressures

A first series of experiments was performed at a silver plate cathode using K₂SO₄ as supporting electrolyte, since this salt according to the literature [36, 63, 64] can give quite good results in terms of CO production and it grants a quite high conductivity. In particular, a series of polarizations and pseudo-polarizations was achieved both at 1 bar and under pressure to achieve information on the process. Afterwards, a series of electrolyses was performed at different CO₂ pressures, current densities and mixing rates.

Figure 1a reports some polarizations recorded under nitrogen or carbon dioxide atmosphere (1 bar) at a silver plate electrode at 0 and 500 rpm. Under nitrogen atmosphere, current density starts to increase significantly at a working potential close to -1.65 V vs. SCE as a result of the hydrogen evolution reaction (HER). When N₂ is replaced with CO₂ at 0 rpm, the current density starts to increase significantly at a working potential close to -1.45 V vs. SCE, thus showing that there is a range of potential of about 0.2 V where CO₂ reduction can potentially take place with a very limited hydrogen evolution. For working potentials more negative than -1.7 V vs SCE (when hydrogen evolution takes place in a relevant way), the addition of CO₂ gives rise to a decrease of the overall current density. The difference between the overall current and the current recorded in the absence of CO₂ was called $j_{\text{CO}_2\text{-N}_2}$ and it is reported in Fig. 1b as a function of the working potential. It is seen that $j_{\text{CO}_2\text{-N}_2}$ presents

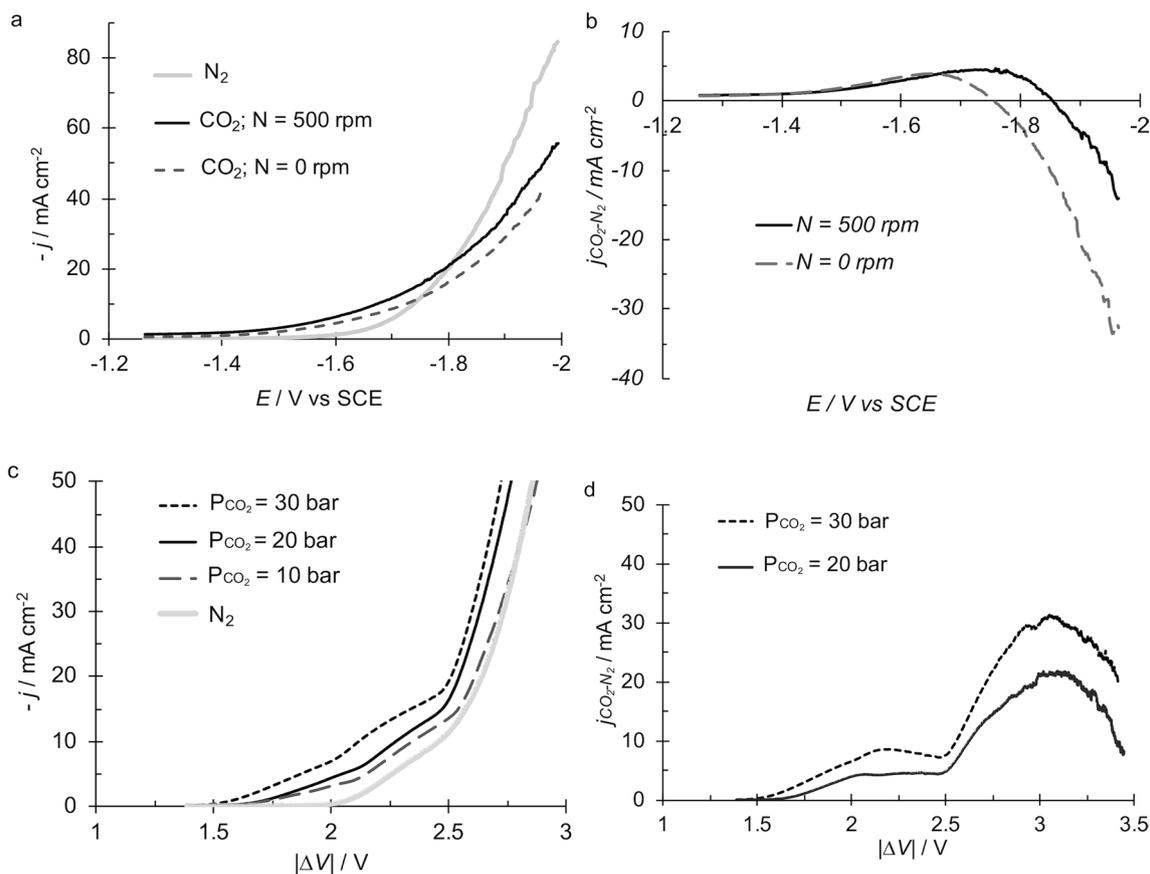
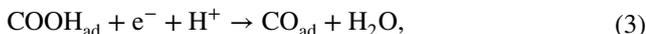


Fig. 1 **a** LSVs at 5 mV s^{-1} under N_2 and CO_2 saturated water solution of $0.2 \text{ M K}_2\text{SO}_4$ at different mixing rate (0 and 500 rpm); the relative polarizations were performed using system I. **b** Plot of $j_{\text{CO}_2-\text{N}_2}$ vs working potential at 0 and 500 rpm; **c** pseudo-polarization curves performed at 5 mV s^{-1} under N_2 and CO_2 saturated water solution of

$0.2 \text{ M K}_2\text{SO}_4$ at different CO_2 pressure (1–30 bar); the relative polarizations were performed using system II. **d** Plot of $j_{\text{CO}_2-\text{N}_2}$ vs cell potential at 20 and 30 bars. Working electrode: plate-Ag (0.1 cm^2). $V=0.05 \text{ L}$

positive values for potentials up to -1.77 V (with a maximum at -1.67 V) and negative values for more negative potentials. Hence, it can be inferred that the addition of CO_2 reduces the rate of hydrogen evolution at least for very negative potentials. According to Hori [17] and Ma [22], the reduction of carbon dioxide at silver cathode proceeds through the formation of adsorbed CO_2^- (Eqs. (1)–(4) where * indicates a free active site).



Conversely, Rosen and co-authors [65] considered that CO_2 and CO_2^- present no stable interactions with Ag, thus

making unlikely that these species can be adsorbed at Ag cathodes. Hence, they proposed the direct formation of COOH_{ad} in the presence of HCO_3^- :



Hence, the decrease of the current in the presence of CO_2 may be related to the fact that the reduction derivatives of carbon dioxide are adsorbed on the silver surface (CO_{ad} , $\text{CO}_{2-\text{ad}}$ and/or COOH_{ad}), thus reducing the active sites for hydrogen evolution reaction.

When polarization was repeated at 500 rpm, an increase of current density was obtained for potentials more negative than -1.6 V (Fig. 1a); this is probably due to the fact that a faster mass transfer of CO_2 and protons favors the CO production. To evaluate the effect of the aqueous concentration of CO_2 on its reduction, current densities were recorded as a function of cell potential ΔV in the presence of N_2 or with different pressures of CO_2 in the range 10–30 bar. As shown in Fig. 1c, current density increases upon enhancing

the CO_2 pressure, thus showing that the rate of carbon dioxide reduction strongly depends on the concentration of CO_2 in solution. Hence, the process is likely to be kinetically limited by the mass transfer of CO_2 from the bulk to the electrode surface and/or its reduction (Eqs. (1) or (5)). However, the limiting current density for direct CO_2 electroreduction can be estimated to be more than 400 mA cm^{-2} at 20 bars under operative conditions adopted in our electrochemical cell. Hence, it can be ruled out the role of mass transfer as r.d.s. at relatively high pressures of carbon dioxide. As shown in Fig. 1d, the plot $j_{\text{CO}_2\text{-N}_2}$ vs. ΔV can be divided in two regions: (I) a first area for ΔV less negative than 2.5 V where the CO_2 evolution takes place in the presence of a small hydrogen evolution and $j_{\text{CO}_2\text{-N}_2}$ tends to a plateau value for more negative potentials; (II) a second area for cell potentials more negative than -2.5 V (where hydrogen evolution starts to take place with a high slope in Fig. 1c) where $j_{\text{CO}_2\text{-N}_2}$ starts again to increase with the potential reaching a maximum value, where carbon dioxide and water reduction coexist and compete.

A series of galvanostatic electrolyses was performed at a silver plate cathode at 12 mA cm^{-2} , 500 rpm and different CO_2 pressures (from 1 to 30 bar) to evaluate the effect of CO_2 concentration on the production of CO and other by-products. As shown in Fig. 2a, according to the literature, at 1 bar CO was produced with a very low CE ($\sim 5\%$), which corresponds to a current density devoted to CO production lower than 0.6 mA cm^{-2} . Indeed, various authors have previously reported that quite low faradic efficiencies and current densities related to CO production are obtained at 1 bar at Ag foil cathodes [66, 67]. The presence of other products of CO_2 reduction, including formic acid, was checked with no results, while a high amount of hydrogen was generated. This result explains once more why several researchers have tried to find alternative solutions such as the use of high

surfaces electrodes or GDE. However, when the pressure was increased, a strong enhancement of the CO production was observed. Indeed, the CE_{CO} increased to 16, 26 and 67% enhancing the CO_2 pressure at 10, 15 and 30 bar, respectively, thus confirming that the enhancement of the CO_2 concentration in the bulk is effective to assist the electrocatalytic properties of silver for the CO generation. Furthermore, at 15 and 30 bars, the presence of small amounts of formic acid in the liquid phase was observed.

One of the main disadvantages of the utilization of an undivided cell is the potential degradation of cathodic products to the anode surface; in this frame, it is important to highlight that our apparatus works in continuous gas-flow mode avoiding gas products accumulation and the potential cathodic reduction of CO. Indeed, the sum of the current efficiency of the cathodic products (CO, H_2 and HCOOH) was close to 100%

3.2 Effect of current density and mixing rate with pressurized carbon dioxide

The effect of current density was evaluated at both 1 and 30 bars, carrying out a series of electrolyses at 7, 12 and 30 mA cm^{-2} and 500 rpm. As shown in Fig. 2b, at 1 bar a very low CO production rate was achieved at all adopted current densities. Conversely, at 30 bar a strong effect of the current density was observed; indeed, the enhancement of the current density from 7 to 12 mA cm^{-2} resulted in a drastic increase of the CO production (from 0.2 to $1.5 \text{ mol h}^{-1} \text{ m}^{-2}$). However, a further enhancement of the current density from 12 to 30 mA cm^{-2} resulted in a slightly increase of CO production accompanied by a drastic decrease of CE_{CO} (from about 65 to 38%). The effect of the current density can be due to the fact that the increase of the current density to 30 mA cm^{-2} involves quite high ΔV

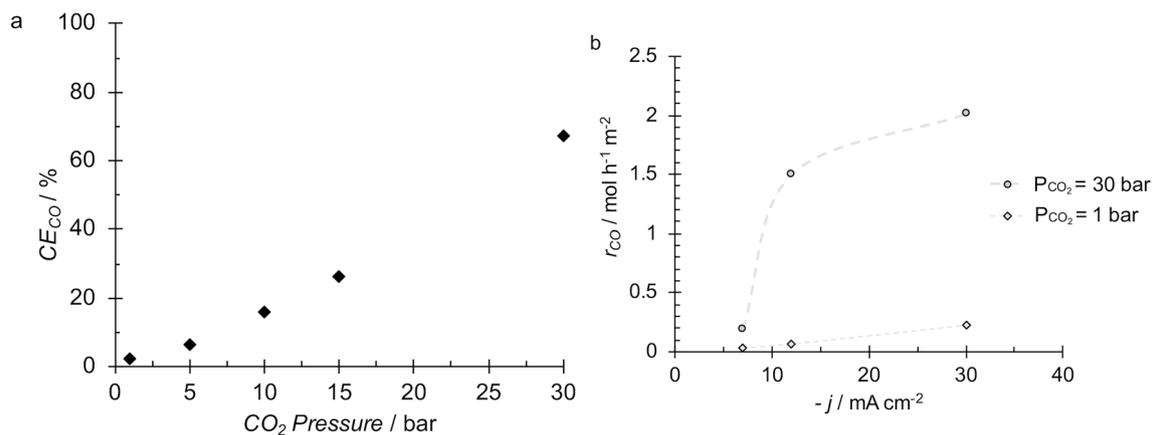


Fig. 2 a Effect of the pressure of CO_2 on the current efficiency of CO at 12 mA cm^{-2} . b Effect of current density on the CO production rate at 1 and 30 bars. Electrolyses were performed in CO_2 saturated water solution of $0.2 \text{ M K}_2\text{SO}_4$ under amperostatic condition

(7–30 mA cm^{-2}). System II. Time: 1 h. Working electrode: Ag plate (3 cm^2). Counter electrode: compact graphite. $N=500 \text{ rpm}$. $V=0.05 \text{ L}$

(~ 2.6 V) that enhance significantly the hydrogen evolution (Fig. 1c) and that, according to some authors, can limit the CO production since at these potentials CO could be more strongly adsorbed to the silver surface due to the back-donation of an electron to the CO specie [47].

To evaluate the effect of mixing on the performances of the process, a series of electrolyses was carried out at 30 bar and 12 mA cm^{-2} at different mixing rates (namely 0, 150, 300, 500 and 700 rpm). In this case, experiments were prolonged up to 3 h. It was shown that CE_{CO} reaches a maximum for an intermediate value of 300 rpm (Fig. 3). Indeed, for higher values of rpm, CE_{CO} decreases as a result of a higher generation of hydrogen. Conversely, for the lower values of the mixing rate, lower current efficiencies for hydrogen are achieved and it was observed a little amount of methane with a current efficiency of about 4%. These results show that under particular operative conditions the reduction of CO_2 at silver can give rise to the formation of methane. The formation of methane at silver plate cathode was previously reported by He [68] and Kuhl [69] in a divided cell using KHCO_3 as supporting electrolyte in the catholyte with current efficiencies lower than 4%. Other studies have shown that, at high pressure, the mixing rate can affect the process; indeed, working without mixing rate gave at copper-based cathodes higher CE in light hydrocarbons [38]. In order to understand the effect of mixing rate on the selectivity of the process, it is relevant to observe that under adopted operating conditions (high pressures of CO_2 and moderate current densities), the reduction of carbon dioxide is not expected to be affected by the mass transfer of CO_2 from the bulk to the cathode surface. Conversely, the mixing rate could affect the mass transfer of CO from the cathode to the bulk. Hence,

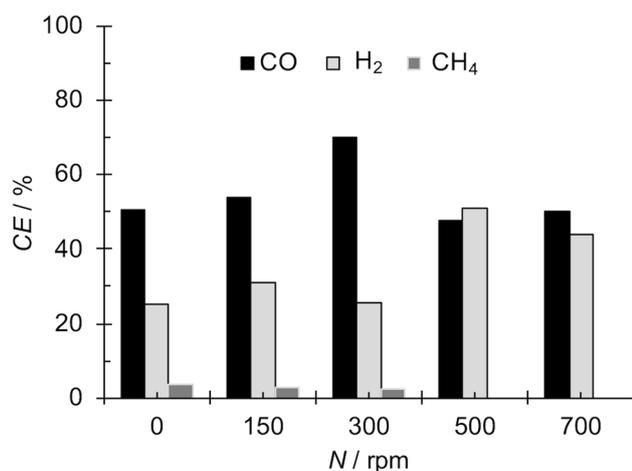


Fig. 3 Effect of the mixing rate on the faradaic efficiency of CO, H₂ and CH₄. Electrolysis were performed in CO_2 saturated water solution of 0.2 M K_2SO_4 under amperostatic condition (12 mA cm^{-2}) at 30 bars. System II. Time: 3 h. Working electrode: Ag plate (3 cm^2). Counter electrode: compact graphite. $V=0.05 \text{ L}$

at low stirring rate, the cathode should present a higher concentration of CO, thus favoring follow-up reduction paths, including the conversion of CO to methane. High stirring rate, furthermore, should enhance the mass transfer of protons from the bulk to the cathode surface, thus decreasing the local pH, and favoring the hydrogen evolution.

3.3 Effect of the supporting electrolyte at different CO_2 pressure and of the anode

The effect of the nature of the supporting electrolyte on the cathodic reduction of CO_2 at silver-based cathodes was evaluated at atmospheric pressure by several authors [31, 70, 71]. In particular, Verma and co-authors [71] have studied that effect of the nature of the supporting electrolyte on the reduction of CO_2 on Ag based GDEs using KOH, KCl and KHCO_3 and have found the higher production of CO with KOH. To evaluate the effect of the nature of the supporting electrolyte on the reduction of pressurized CO_2 to CO at silver cathode, some electrolyses were performed replacing K_2SO_4 with KOH, KCl and KHCO_3 that, according to the literature, allow to achieve good productivity of CO. In the case of KOH some polarizations were also performed.

Table 1 reports the results achieved after 2 h at 1 and 15 bars with the different adopted supporting electrolytes using a silver plate cathode under amperostatic conditions (12 mA cm^{-2}). As shown in Table 1 (entries 1–3) at 1 bar, for all adopted electrolytes, using a compact graphite anode as counter electrode very low current efficiencies in CO were recorded ($< 5\%$). At the end of electrolyses, the presence in solution of small particles of compact graphite, generated by the deterioration of the anode, was observed.

Hence, the electrolyses with KOH and KCl were repeated using a dimensional stable electrode $\text{Ti}/\text{IrO}_2\text{-Ta}_2\text{O}_5$ as anode. In both cases, higher CE_{CO} were obtained (Table 1, entries 4 and 5), even if always lower than 10%. When experiments were repeated at 15 bars (Table 1, entries 6–8), the productions of CO increased for all the adopted supporting electrolytes, thus confirming the beneficial effect of CO_2 pressure on the cathodic reduction of carbon dioxide.

Furthermore, a strong effect of the nature of the supporting electrolyte on the performances of the process was observed. In particular, with K_2SO_4 and KCl, at 15 bars (Table 1, entries 6 and 7) quite similar CE_{CO} were obtained (44 and 39%), while with KOH and KHCO_3 (Table 1, entries 8 and 9), a higher production of CO was obtained (CE_{CO} of 60 and 65%). together with a lower cell potential. In particular, the energetic consumption decreased of about 50% using KOH and KHCO_3 (0.24 and 0.27 kWh/mol_{CO} for KOH and KHCO_3 , respectively) instead of the other two supporting electrolytes (about 0.4 kWh/mol_{CO}), because of both the higher CE_{CO} and the lower cell potential recorded with these salts. In our system, where carbon dioxide is continuously

Table 1 Effect of supporting electrolyte on the CO₂ reduction to CO at different CO₂ pressures

Entry	Supporting electrolyte ^a	Counter electrode	CO ₂ pressure / bar	Cell potential / V	E / V vs SCE	pH final	CE _{CO} / %	r _{CO} / mol h ⁻¹ m ⁻²	Energetic consumption / kWh/mol _{CO}	EE _{CO} / %
1	K ₂ SO ₄	Graphite	1	4.00	-2.00	5.5	<3	0.07	7.20	1.0
2	KCl	Graphite	1	3.30	-1.80	5.5	<3	0.06	7.10	1.6
3	KOH	Graphite	1	3.45	-1.65	7.2	4	0.09	4.70	1.5
4	KOH	DSA	1	3.30	-1.75	7	9.8	0.22	1.80	3.9
5	KCl	DSA	1	3.30	-1.70	5.5	7	0.16	2.60	2.8
6	K ₂ SO ₄	DSA	15	3.08	NA	5-5.5	44	1.00	0.35	20.5
7	KCl	DSA	15	3.05	NA	5.5	39	0.87	0.42	17.3
8	KOH	DSA	15	2.85	NA	7.3	65	1.46	0.24	30.3
9	KHCO ₃	DSA	15	3.00	NA	7.4	60	1.36	0.27	26.6

Electrolyses were performed under amperostatic conditions (12 mA cm⁻²). System I was used for electrolyses at ambient pressure, System II was used for electrolyses at 20 bars. Working electrode: plate-Ag. N = 500 rpm. V = 0.05 L

NA not available

^aConcentration: 0.2 M K₂SO₄; 0.5 M KCl, KHCO₃ or KOH

fed to the system, H₂CO₃ is expected to react with KOH to give KHCO₃, thus giving rise to the formation of a buffer solution. Hence, similar results are expected using KOH or KHCO₃. Indeed, these two electrolytes gave the highest values of CE_{CO}. The slightly higher production of CO achieved in the presence of KOH could be due to various reasons such as transient effects, even if the saturation of the solution with CO₂ for 30 min before the electrolysis should reduce the not-stationary period, or a surface modification of silver electrode when it is immersed in KOH aqueous solution.

The reduction of CO₂ at silver in the presence of KOH was further investigated by polarization studies. Figure 4a reports the polarizations achieved using KOH or K₂SO₄ under nitrogen and carbon dioxide atmosphere (1 bar). Similar forms of the polarizations were achieved at the two electrolytes. However, with KOH higher current densities were recorded both under N₂ and in CO₂ atmosphere (Fig. 4a, b). In particular, when KOH is used the replacement of N₂ with CO₂ gives rise to an increase of the current density for working potentials up to -1.7 V vs. SCE, when the hydrogen evolution is limited: hence, there is a range of potential (from -1.3 to -1.7 V) where hydrogen evolution is very limited and CO₂ reduction can take place. Conversely, for working potential more negative than -1.7 V (when hydrogen evolution takes place in a relevant way), the addition of CO₂ gives rise to a decrease of the overall current density. As previously observed for experiments performed with K₂SO₄, this is probably due to the fact that the derivatives of carbon dioxide reduction are adsorbed at silver, thus reducing the active sites for water reduction, or to the depletion of protons at the cathode surface driven by CO formation. As shown in Fig. 4c, when the pressure of CO₂ is enhanced from 1 to 20 bar, a significant increase of the current density is observed, thus showing that the rate of carbon dioxide reduction depends on the concentration of CO₂ also using KOH. However, when the pressure is increased from 20 to 30 bar, no a significant change of the current densities was observed, thus showing that at these relatively high pressures, the process is no more affected by the concentration of CO₂ in the bulk. It was also shown that higher current densities are recorded for KOH with respect to K₂SO₄ for each value of the pressure and of the cell potential (Figs. 1c and 4c), according to the above-mentioned results and considerations.

3.4 Effect of the nature of cathode

The silver plate cathode (named plate-Ag) is characterized by a quite low specific surface. Hence, in order to increase the performances of the process some polarizations, pseudo-polarizations and electrolyses were repeated in the presence of a high surface Ag based electrode (hs-Ag).

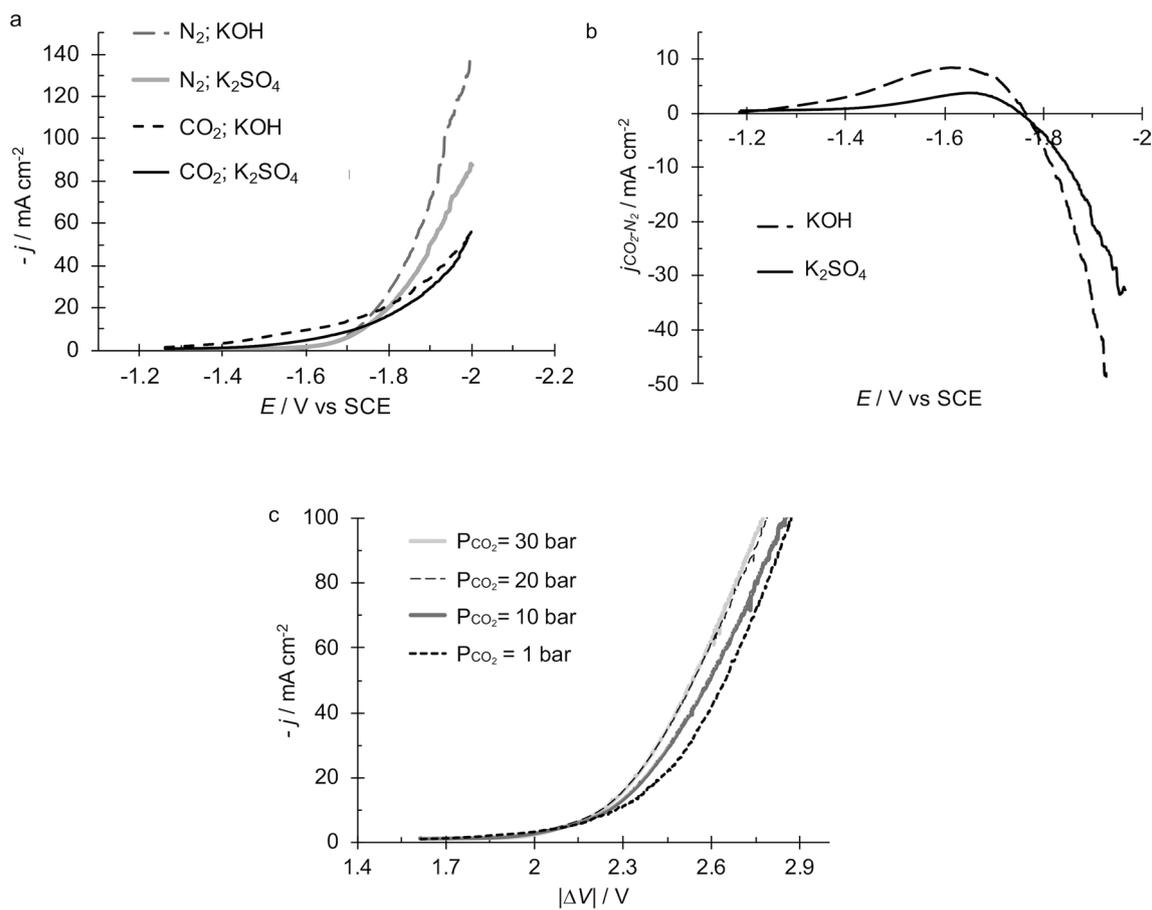


Fig. 4 **a** LSVs at 5 mV s^{-1} under N_2 and CO_2 saturated water solution of $0.2 \text{ M K}_2\text{SO}_4$ or 0.5 M KOH ; the relative polarizations were performed using system I. **b** Plot $j^{\text{CO}_2\text{-N}_2}$ vs working potential using KOH and K_2SO_4 . **c** Pseudo-polarization curves performed

at 5 mV s^{-1} under CO_2 saturated water solution of 0.5 M KOH at different CO_2 pressure (1–30 bar). The relative polarizations were performed using system II. Working electrode: plate-Ag (0.1 cm^2). $V=0.05 \text{ L}$

3.4.1 Polarizations and pseudo-polarization measurements

Figure 5a reports some polarization curves recorded with the two cathodes. Under nitrogen atmosphere, high apparent current densities are recorded for hs-Ag, probably for the higher surface due to the occurrence of pore structure. However, at the more negative working potentials the polarizations achieved at the two electrodes become more similar. This behavior could be due to the fact that for very negative working potential, the massive hydrogen evolution could fill the pores, limiting the active surface available for water reduction. Under carbon dioxide atmosphere, the CO_2 reduction starts at similar potentials at the two electrodes, but a strong increase of the current density is recorded for hs-Ag with respect to plate-Ag, thus showing that the higher surface of hs-Ag can be exploited for CO_2 reduction.

Figure 5b reports the value of $j^{\text{CO}_2\text{-N}_2}$ achieved at the two cathodes in the absence and in the presence of mixing. It is shown that at both electrodes, $j^{\text{CO}_2\text{-N}_2}$ presents a

slight increase in the presence of the mixing, thus showing that at 1 bar the process is partially limited by the mass transfer of CO_2 to the cathode surface for both electrodes. Figure 5c reports the pseudo-polarizations achieved at the two cathodes at various CO_2 pressures. It is shown that (i) hs-Ag gives higher current densities with respect to plate-Ag at all adopted pressures and (ii) a smaller effect of pressure is observed for hs-Ag, thus showing that at this electrode the rate determining step, at least at pressure higher than 10 bar, depends in a limited way on the CO_2 concentration in the bulk.

3.4.2 Electrolyses

As shown in Table 2, the replacement of the plate-Ag cathode with the hs-Ag one allowed to achieve a strong increase of CO production by amperostatic electrolyses at 1 bar and 12 mA cm^{-2} ; indeed, the CE_{CO} were about 10 and 31% at

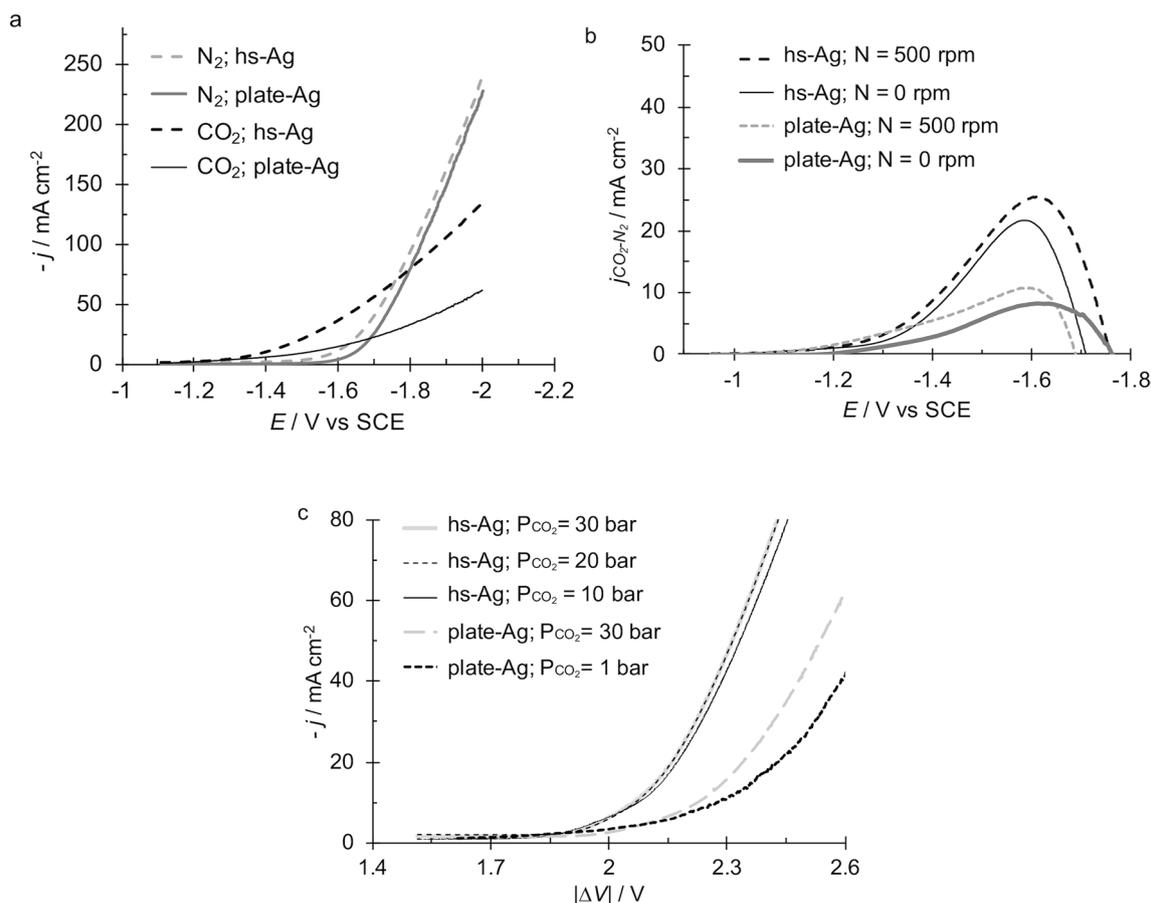


Fig. 5 **a** LSVs at 5 mV s⁻¹ under N₂ and CO₂ saturated water solution of 0.5 M KOH at two different electrodes: plate silver (plate-Ag) and a high surface silver electrode (hs-Ag) at 500 rpm; the relative polarizations were performed using system I. **b** Plot of $j_{\text{CO}_2\text{-N}_2}$ vs. working potential at 0 and 500 rpm of the plate-Ag and hs-Ag cath-

odes. **c** Pseudo-polarization curves performed at 5 mV s⁻¹ under CO₂ saturated water solution of 0.5 M KOH at different CO₂ pressure (1–30 bar) using System II and at two different electrodes: plate-Ag and hs-Ag cathode. System II. $A_{\text{cathode}} = 0.1 \text{ cm}^2$. $V = 0.05 \text{ L}$

the plate-Ag and hs-Ag cathodes (Table 2, entries 1 and 3). In particular, at hs-Ag cathode the same value of current density was achieved with a lower value of the working potential, according with the pseudo-polarization curves reported in Fig. 5, thus allowing to reduce the impact of water reduction.

To evaluate the effect of current density on the production of CO at the hs-Ag cathode, a series of amperostatic electrolyses was carried out at 1 bar and 12, 36 and 50 mA cm⁻². As shown in Table 2, at all adopted current densities, the replacement of plate-Ag (entries 1 and 2) with hs-Ag (3 and 4) gave rise to an enhancement of about three times of the CE_{CO} and allowed to achieve a significant decrease of working and cell potentials. This is due to the fact that at low concentrations of carbon dioxide, the high surface of hs-Ag allows to speed up the process. Focusing on hs-Ag cathode, the enhancement of the current density from 12 to 36 mA cm⁻² (Table 2, entries 3 and 4) resulted

in a strong increase of the CO production (from 0.69 to 1.61 mol h⁻¹ m⁻²) as a result of the higher amount of charge passed, even if with a decrease of the CE_{CO} from 31 to 24%, probably due to an increase of the hydrogen evolution due to the more negative working potential involved. When the current density was further increased to 50 mA cm⁻² (Table 2, entry 5), the production of CO decreased, with a dramatic reduction of CE_{CO} to 9%, due to the occurrence of a quite negative working potential (-2.35 V vs SCE) that can favor the HER and decrease the CO desorption, as above discussed [47].

In order to evaluate the effect of the pressure on the process at the high surface cathode, a series of electrolyses was performed at different pressures (1, 10, 20 and 30 bar) and current densities (12, 36 and 50 mA cm⁻²) at hs-Ag cathode. At 12 mA cm⁻², an increase of the pressure from 1 to 20 bars did not affect the performances of the process (Table 3, entry 1 and 2), according to the pseudo-polarization curves;

Table 2 Effect of cathode and supporting electrolyte on the performance of the CO₂ reduction to CO

Entry	Cathode	Supporting electrolyte / 0.5 M	Current density / mA cm ⁻²	CO ₂ pressure / bar	Cell potential / V	E / V vs SCE	pH final	CE _{CO} / %	r _{CO} / mol h ⁻¹ m ⁻²	Energetic consumption / kWh / mol _{CO}	EE _{CO} / %
1	Plate-Ag	KOH	12	1	3.30	-1.75	7.0	9.8	0.22	1.83	3.9
2	Plate-Ag	KOH	36	1	4.90	-2.15	7.0	8.1	0.54	3.30	2.2
3	hs-Ag	KOH	12	1	2.86	-1.60	7.3	31.0	0.69	0.50	14.7
4	hs-Ag	KOH	36	1	4.00	-2.00	7.1	24.0	1.61	0.90	8.2
5	hs-Ag	KOH	50	1	5.20	-2.35	7.3	9.0	0.84	3.10	2.3
6	plate-Ag	KOH	36	20	4.10	NA	7.2	50.0	3.36	0.44	16.2
7	hs-Ag	KOH	36	20	3.50	NA	7.3	57.8	3.90	0.32	22.0

Electrolyses were performed using a DSA as counter electrode under amperostatic conditions. System I was used for electrolyses at ambient pressure, System II was used for electrolyses at 20 bars. *N* = 500 rpm. *V* = 0.05 L, KOH was used as supporting electrolyte

NA not available

indeed, a value of CE_{CO} of about 30% was achieved at both 1 and 20 bars, probably due to the fact that, under adopted operative conditions, the r.d.s. does not involve the mass transport of CO₂ or its cathodic reduction. Conversely, at 36 and 50 mA cm⁻², a strong effect of the pressure was observed; indeed, as an example, an increase of the pressure from 1 to 10 and 20 bar at 36 mA cm⁻² resulted in a simultaneously reduction of the cell potential of about 115 and 550 mV, respectively, and in an enhancement of CE_{CO} from 24 up to 40 and 57% (Table 3, entries 3–5), probably due to the fact that at high current densities and working potentials the process becomes kinetically limited by the concentration of CO₂. Indeed, as shown in Fig. 5b, at these values of current density and cell potentials, the current increases enhancing the pressure from 10 to 20 bars.

However, a further increase of the pressure from 20 to 30 bars resulted in a slightly decrease of the CE_{CO} (from 57 to at 50%) and in a very small change of the total CO₂ reduction efficiency (computed taking in account the CO and the formic acid formation), which was close to 59% at both 20 and 30 bars, according to the pseudo-polarizations reported in Fig. 5b, because the concentration of carbon dioxide in the bulk at these high pressures becomes sufficient to sustain the mass transport and the cathodic reduction of CO₂ and the process is likely to be limited by a following step, similarly to what observed at low current densities.

The performances of hs-Ag and plate-Ag at high pressures are compared in Table 2. The increase of the pressure from 1 to 20 bar (entries 2, 4, 8 and 9) allowed to increase drastically both the CO production and the corresponding CE_{CO} at both electrodes (from 8 to 50% at plate-Ag and from 24 to 58% at hs-Ag). However, at high pressures, the benefits of using hs-Ag is less important (CE_{CO} 50% at plate-Ag and 58% at hs-Ag), because the high solubility of CO₂ achieved at high pressures makes less relevant the surface of the cathode. These results seem quite important because it shows that relatively high pressures can allow to avoid the use of more complex and expensive electrodes.

3.5 Time stability of performances at high pressure

To evaluate the stability of the performances of the process, two long amperostatic electrolyses were performed at plate-Ag with both KOH and K₂SO₄ electrolytes at 15 bar and 12 mA cm⁻² (Fig. 6). It was shown that the process takes place under very stable conditions in terms of production of CO, CE_{CO} and cell potential using KOH as supporting electrolyte; indeed, a CE_{CO} close to 70% was recorded for 10 h for a very stable value of the cell potential. Conversely, for K₂SO₄, the CE_{CO} presented a small decrease from 53 to 45% after 2 h, a period of stability for about 6 h and a decrease for the last 3 h to reach a value close to 20% after 10 h and a correspondent increase of the cell potential up to 3.2 V,

Table 3 Effect of the pressure at hs-Ag cathode on the performances of the CO₂ reduction to CO

Entry	CO ₂ pressure / bar	Current density / mA cm ⁻²	Cell potential / V	pH final	CE _{CO} / %	r _{CO} / mol h ⁻¹ m ⁻²	Energetic consumption / kWh/mol _{CO}	EE _{CO} / %
1	1	12	2.86	7.3	31.0	0.69	0.50	14.4
2	20	12	2.75	7.4	28.5	0.64	0.52	13.5
3	1	36	4.00	7.1	24.0	1.61	0.90	8.0
4	10	36	3.87	7.0	40.3	2.71	0.52	13.8
5	20	36	3.45	7.4	57.8	3.90	0.32	22.3
6	30	36	3.30	7.4	49.5	3.32	0.36	20
7	1	50	5.20	7.3	9.0	0.84	3.10	2.3
8	20	50	3.80	7.4	49.0	4.57	0.41	17.1

Electrolysis were performed in water solution of 0.5 M KOH under amperostatic conditions. System I was used for electrolyses at ambient pressure, System II was used for electrolyses at 10, 20 and 30 bars. Working electrode: hs-Ag. Counter electrode: DSA®. *N* = 500 rpm. *V* = 0.05 L

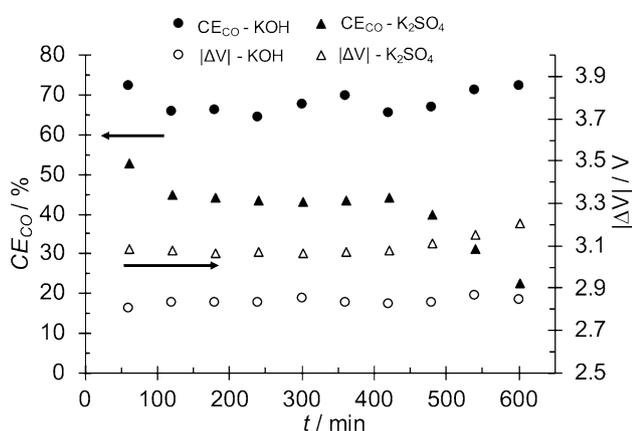


Fig. 6 Effect of the time on the current efficiency of CO under pressurized condition ($PCO_2 = 15$ bar). Electrolysis was performed in water solution of 0.5 M KOH or 0.2 M K_2SO_4 at 12 mA cm^{-2} . System II. Working electrode: Ag plate (3 cm^2). Counter electrode: DSA®. *N* = 500 rpm. *V* = 0.05 L

potentials values in which CO₂ and water reduction coexist and compete, thus limiting the CO₂ reduction.

4 Conclusions

Electrochemical conversion of CO₂ to CO at silver electrodes was studied in detail using a liquid phase electrolyzer, investigating the effect of several operating parameters, including CO₂ pressure (1–30 bar), nature of supporting electrolytes and current density. It was found that a simple and relatively cheap undivided cell equipped with simple silver sheet cathodes can allow to obtain interesting current efficiency in CO (CE_{CO}) using pressurized conditions at medium current densities. For example, at silver plate electrode and 12 mA cm^{-2} , the current efficiency of CO

dramatically increases from really low values (< 4%) at 1 bar to 67% at 30 bars. Furthermore, it was found that:

- the effect of the surface of the electrode strongly depends on the adopted CO₂ pressure. At 1 bar the increase of the surface allows to improve strongly the performances of the process; as an example, the replacement of the plate Ag electrode with a high surface one allows to increase the CE_{CO} from 8 to 24% at 36 mA cm^{-2} . However, at 20 bar the effect of the surface is reduced; indeed, the replacement gave rise to a quite small improvement of the CE_{CO} from 50 to 57% at plate and high surface Ag electrode, respectively, at 36 mA cm^{-2} ;
- there is an important effect of the nature of the supporting electrolyte at high pressure. Indeed, at 15 bars, a higher production of CO with a quite high current efficiency of about 60–65% was reached by replacing K_2SO_4 or KCl (both $CE_{CO} \sim 40\%$) with KOH or $KHCO_3$ at silver plate cathode and 12 mA cm^{-2} ;
- at high pressure, the mixing rate can affect the product distribution even if mass transfer control of CO₂ electroreduction can be excluded; in particular, under particular operative conditions, the reduction of CO₂ gives rise to the formation of CH₄ even if with low current efficiency (4%);
- the effect of current density strongly depends on both the adopted pressure and surface of the electrode. In particular, the productivity of the system can be increased, by enhancing the current density, using (i) high pressure of CO₂ or (ii) high surface electrodes.

Furthermore, the stability of the performances highly depends on the adopted operating conditions. In particular, the process was stable with the time maintaining a quite high current efficiency for CO of about 70% for 10 h using mild

pressure (15 bar), a simple plate silver electrode and KOH as supporting electrolyte.

On the overall, the results reported in this manuscript demonstrate that the utilization of carbon dioxide at mild pressure allows to operate with simple electrodes in undivided cells by maintaining quite good results. In this context, it is worth to mention that, according to several authors [58, 59], the utilization of pressurized conditions up to 20 bars does not impact remarkably on the global costs of the process, involving just a small increase of operative and capital costs with respect the other main costs. Conversely, it has been shown the implementation of CO₂ reduction technologies on large scale is mainly limited by the electrolyzer costs (almost 50% of the overall costs) [72–74], predominantly due to the energy consumption and GDE costs (e.g. estimated GDE cost of about 7700 € m⁻² [75]).

From the industrial point of view, the utilization of pressurized conditions could be an interesting alternative to the direct integration of the pressurized products' streams (i.e. syngas) as a feedstock with other conventional industrial processes currently performed at high pressure. In this framework, further investigations will be necessary to improve the scalability on large scale of this apparatus. Indeed, this process may suffer of the potential formation of an explosive mixture of H₂ and O₂ and of a low CO₂ utilization rate; hence, further researches will be focused on this topic and various strategies will be tested, including: (i) the implementation of sacrificial anodes to avoid the O₂ evolution reaction; (ii) the utilization of higher-selective CO 3D-cathodes (mesh, perforated, foam) to suppress the H₂ production and improve the CO productivity at high pressure; (iii) the development of a novel reactor configuration operating in continuous mode, in order to prevent the mixing of potentially formed cathodic co-product, hydrogen, with the anodic product, oxygen and to increase the conversion rate. It is worth to mention that a similar alternative to the latter was successfully evaluated by some authors [36, 55], which have estimated an improvement of the CO₂ conversion rate up to 26% and an enhancement of the selectivity towards CO using a divided semi-continuous mode system under pressurized conditions.

Acknowledgements University of Palermo is acknowledged for its financial support.

Funding Open access funding provided by Università degli Studi di Palermo within the CRUI-CARE Agreement.

Compliance with ethical standards

Conflict of interest The authors declare that they have no conflict of interest.

Open Access This article is licensed under a Creative Commons Attribution 4.0 International License, which permits use, sharing, adaptation, distribution and reproduction in any medium or format, as long as you give appropriate credit to the original author(s) and the source, provide a link to the Creative Commons licence, and indicate if changes were made. The images or other third party material in this article are included in the article's Creative Commons licence, unless indicated otherwise in a credit line to the material. If material is not included in the article's Creative Commons licence and your intended use is not permitted by statutory regulation or exceeds the permitted use, you will need to obtain permission directly from the copyright holder. To view a copy of this licence, visit <http://creativecommons.org/licenses/by/4.0/>.

References

1. Verma S, Kim B, Jhong HRM et al (2016) A gross-margin model for defining technoeconomic benchmarks in the electroreduction of CO₂. *Chemsuschem* 9:1972–1979. <https://doi.org/10.1002/cssc.201600394>
2. Agarwal AS, Zhai Y, Hill D, Sridhar N (2011) The electrochemical reduction of carbon dioxide to formate/formic acid: engineering and economic feasibility. *Chemsuschem* 4:1301–1310. <https://doi.org/10.1002/cssc.201100220>
3. Higgins D, Hahn C, Xiang C et al (2019) Gas-diffusion electrodes for carbon dioxide reduction: a new paradigm. *ACS Energy Lett* 4:317–324. <https://doi.org/10.1021/acsenergylett.8b02035>
4. Bushuyev OS, De LP, Dinh CT et al (2018) What should we make with CO₂ and how can we make it? *Joule* 2:1–8. <https://doi.org/10.1016/j.joule.2017.09.003>
5. Jhong HRM, Ma S, Kenis PJ (2013) Electrochemical conversion of CO₂ to useful chemicals: current status, remaining challenges, and future opportunities. *Curr Opin Chem Eng* 2:191–199. <https://doi.org/10.1016/j.coche.2013.03.005>
6. Kibria MG, Edwards JP, Gabardo CM et al (2019) Electrochemical CO₂ reduction into chemical feedstocks: from mechanistic electrocatalysis models to system design. *Adv Mater* 31:1807166. <https://doi.org/10.1002/adma.201807166>
7. Zheng T, Jiang K, Ta N et al (2019) Large-scale and highly selective CO₂ electrocatalytic reduction on nickel single-atom catalyst. *Joule* 3:265–278. <https://doi.org/10.1016/j.joule.2018.10.015>
8. Birdja YY, Koper MTM (2017) The importance of cannizzaro-type reactions during electrocatalytic reduction of carbon dioxide. *J Am Chem Soc* 139:2030–2034. <https://doi.org/10.1021/jacs.6b12008>
9. Kim Y, Trung TSB, Yang S et al (2016) Mechanism of the surface hydrogen induced conversion of CO₂ to methanol at Cu(111) step sites. *ACS Catal* 6:1037–1044. <https://doi.org/10.1021/acscatal.5b02083>
10. Alvarez-Guerra M, Del Castillo A, Irabien A (2014) Continuous electrochemical reduction of carbon dioxide into formate using a tin cathode: Comparison with lead cathode. *Chem Eng Res Des* 92:692–701. <https://doi.org/10.1016/j.cherd.2013.11.002>
11. Kopljar D, Inan A, Vindayer P et al (2014) Electrochemical reduction of CO₂ to formate at high current density using gas diffusion electrodes. *J Appl Electrochem* 44:1107–1116. <https://doi.org/10.1007/s10800-014-0731-x>
12. Albo J, Alvarez-Guerra M, Castaño P, Irabien A (2015) Towards the electrochemical conversion of carbon dioxide into methanol. *Green Chem* 17:2304–2324. <https://doi.org/10.1039/C4GC02453B>

13. Del Castillo A, Alvarez-Guerra M, Solla-Gullón J et al (2017) Sn nanoparticles on gas diffusion electrodes: synthesis, characterization and use for continuous CO₂ electroreduction to formate. *J CO₂ Util* 18:222–228. <https://doi.org/10.1016/j.jcou.2017.01.021>
14. Hoang TTH, Verma S, Ma S et al (2018) Nanoporous copper-silver alloys by additive-controlled electrodeposition for the selective electroreduction of CO₂ to ethylene and ethanol. *J Am Chem Soc* 140:5791–5797. <https://doi.org/10.1021/jacs.8b01868>
15. Gennaro A, Isse AA, Severin M-G et al (1996) Mechanism of the electrochemical reduction of carbon dioxide at inert electrodes in media of low proton availability. *J Chem Soc Faraday Trans* 92:3963–3968. <https://doi.org/10.1039/FT9969203963>
16. Scialdone O, Galia A, Errante G et al (2008) Electrocarboxylation of benzyl chlorides at silver cathode at the preparative scale level. *Electrochim Acta* 53:2514–2528. <https://doi.org/10.1016/j.electacta.2007.10.021>
17. Hori Y, Wakabe H, Tsukamoto T, Koga O (1994) Electrocatalytic process of CO selectively in electrochemical reduction of CO₂ at metal electrodes in aqueous media. *Electrochim Acta* 39:1833–1839. [https://doi.org/10.1016/0013-4686\(94\)85172-7](https://doi.org/10.1016/0013-4686(94)85172-7)
18. Hernández S, Farkhondehfal MA, Sastre F et al (2017) Syngas production from electrochemical reduction of CO₂: current status and prospective implementation. *Green Chem* 19:2326–2346. <https://doi.org/10.1039/C7GC00398F>
19. Qiao J, Liu Y, Hong F, Zhang J (2014) A review of catalysts for the electroreduction of carbon dioxide to produce low-carbon fuels. *Chem Soc Rev* 43:631–675. <https://doi.org/10.1039/c3cs60323g>
20. Hu XM, Hval HH, Bjerglund ET et al (2018) Selective CO₂ reduction to CO in water using earth-abundant metal and nitrogen-doped carbon electrocatalysts. *ACS Catal* 8:6255–6264. <https://doi.org/10.1021/acscatal.8b01022>
21. Salehi-Khojin A, Jhong HRM, Rosen BA et al (2013) Nanoparticle silver catalysts that show enhanced activity for carbon dioxide electrolysis. *J Phys Chem C* 117:1627–1632. <https://doi.org/10.1021/jp310509z>
22. Ma M, Trzeźniewski BJ, Xie J, Smith WA (2016) Selective and efficient reduction of carbon dioxide to carbon monoxide on oxide-derived nanostructured silver electrocatalysts. *Angew Chemie - Int Ed* 55:9748–9752. <https://doi.org/10.1002/anie.201604654>
23. Lu Q, Rosen J, Zhou Y et al (2014) A selective and efficient electrocatalyst for carbon dioxide reduction. *Nat Commun* 5:1–6. <https://doi.org/10.1038/ncomms4242>
24. Ma S, Luo R, Gold JI et al (2016) Carbon nanotube containing Ag catalyst layers for efficient and selective reduction of carbon dioxide. *J Mater Chem A* 4:8573–8578. <https://doi.org/10.1039/c6ta00427j>
25. Chen Y, Li CW, Kanan MW (2012) Aqueous CO₂ reduction at very low overpotential on oxide-derived Au nanoparticles. *J Am Chem Soc* 134:19969–19972. <https://doi.org/10.1021/ja309317u>
26. Li CW, Kanan MW (2012) CO₂ reduction at low overpotential on Cu electrodes resulting from the reduction of thick Cu₂O films. *J Am Chem Soc* 134:7231–7234. <https://doi.org/10.1021/ja3010978>
27. Farkhondehfal MA, Hernández S, Rattalino M et al (2019) Syngas production by electrocatalytic reduction of CO₂ using Ag-decorated TiO₂ nanotubes. *Int J Hydrogen Energy*. <https://doi.org/10.1016/j.ijhydene.2019.04.180>
28. Lu Q, Jiao F (2016) Electrochemical CO₂ reduction: electrocatalyst, reaction mechanism, and process engineering. *Nano Energy* 29:439–456. <https://doi.org/10.1016/j.nanoen.2016.04.009>
29. Delacourt C, Ridgway PL, Kerr JB, Newman J (2007) Design of an electrochemical cell making syngas (CO+H₂) from CO₂ and H₂O reduction at room temperature. *J Electrochem Soc* 155:B42–B49. <https://doi.org/10.1149/1.2801871>
30. Yamamoto T, Hirota K, Tryk DA et al (2003) Electrochemical reduction of CO₂ in micropores. *Chem Lett* 27:825–826. <https://doi.org/10.1246/cl.1998.825>
31. Thorson MR, Siil KI, Kenis PJ (2013) Effect of cations on the electrochemical conversion of CO₂ to CO. *J Electrochem Soc* 160:F69–F74. <https://doi.org/10.1149/2.052301jes>
32. Kim B, Ma S, Molly Jhong HR, Kenis PJA (2015) Influence of dilute feed and pH on electrochemical reduction of CO₂ to CO on Ag in a continuous flow electrolyzer. *Electrochim Acta* 166:271–276. <https://doi.org/10.1016/j.electacta.2015.03.064>
33. Kim B, Hillman F, Ariyoshi M et al (2016) Effects of composition of the micro porous layer and the substrate on performance in the electrochemical reduction of CO₂ to CO. *J Power Sources* 312:192–198. <https://doi.org/10.1016/j.jpowsour.2016.02.043>
34. Lister TE, Dufek EJ, Stone SG (2013) Electrochemical systems for production of syngas and co-products. *ECS Trans* 58:125–137. <https://doi.org/10.1149/05802.0125ecst>
35. Wang Q, Dong H, Yu H, Yu H (2015) Enhanced performance of gas diffusion electrode for electrochemical reduction of carbon dioxide to formate by adding polytetrafluoroethylene into catalyst layer. *J Power Sources* 279:1–5. <https://doi.org/10.1016/j.jpowsour.2014.12.118>
36. Jeanty P, Scherer C, Magori E et al (2018) Upscaling and continuous operation of electrochemical CO₂ to CO conversion in aqueous solutions on silver gas diffusion electrodes. *J CO₂ Util* 24:454–462. <https://doi.org/10.1016/j.jcou.2018.01.011>
37. Hara K, Kudo A, Sakata T (1995a) Electrochemical reduction of carbon dioxide under high pressure on various electrodes in an aqueous electrolyte. *J Electroanal Chem* 391:141–147. [https://doi.org/10.1016/0022-0728\(95\)03935-A](https://doi.org/10.1016/0022-0728(95)03935-A)
38. Hara K, Tsuneto A, Kudo A, Sakata T (1994) Electrochemical reduction of CO₂ on a Cu electrode under high pressure: factors that determine the product selectivity. *J Electrochem Soc* 141:2097–2103. <https://doi.org/10.1149/1.2055067>
39. Hara K, Kudo A, Sakata T (1997) Electrochemical CO₂ reduction on a glassy carbon electrode under high pressure. *J Electroanal Chem* 421:1–4. [https://doi.org/10.1016/S0022-0728\(96\)01028-5](https://doi.org/10.1016/S0022-0728(96)01028-5)
40. Hara K, Kudo A, Sakata T (1995b) Electrochemical reduction of high pressure carbon dioxide on Fe electrodes at large current density. *J Electroanal Chem* 386:257–260
41. Dufek EJ, Lister TE, Stone SG, McIlwain ME (2012) Operation of a pressurized system for continuous reduction of CO₂. *J Electrochem Soc* 159:F514–F517. <https://doi.org/10.1149/2.011209jes>
42. Proietto F, Schiavo B, Galia A, Scialdone O (2018) Electrochemical conversion of CO₂ to HCOOH at tin cathode in a pressurized undivided filter-press cell. *Electrochim Acta* 277:30–40. <https://doi.org/10.1016/j.electacta.2018.04.159>
43. Proietto F, Galia A, Scialdone O (2019) Electrochemical conversion of CO₂ to HCOOH at tin cathode: development of a theoretical model and comparison with experimental results. *ChemElectroChem* 6:162–172. <https://doi.org/10.1002/celec.201801067>
44. Scialdone O, Galia A, Lo NG et al (2015) Electrochemical reduction of carbon dioxide to formic acid at a tin cathode in divided and undivided cells: Effect of carbon dioxide pressure and other operating parameters. *Electrochim Acta* 199:332–341. <https://doi.org/10.1016/j.electacta.2016.02.079>
45. Dufek EJ, Lister TE, Stone SG (2014) Sampling dynamics for pressurized electrochemical cells. *J Appl Electrochem* 44:849–855. <https://doi.org/10.1007/s10800-014-0693-z>
46. Gabardo CM, Seifitokaldani A, Edwards JP et al (2018) Combined high alkalinity and pressurization enable efficient CO₂ electroreduction to CO. *Energy Environ Sci* 11:2531–2539. <https://doi.org/10.1039/c8ee01684d>

47. Kudo A, Nakagawa S, Tsuneto A, Sakata T (1993) Electrochemical reduction of high pressure CO₂ on Ni electrodes. *J Electrochem Soc* 140:1541. <https://doi.org/10.1149/1.2221599>
48. Todoroki M, Hara K, Kudo A, Sakata T (1995) Electrochemical reduction of high pressure CO₂ at Pb, Hg and In electrodes in an aqueous KHCO₃ solution. *J Electroanal Chem* 394:199–203. [https://doi.org/10.1016/0022-0728\(95\)04010-L](https://doi.org/10.1016/0022-0728(95)04010-L)
49. DiMeglio JL, Rosenthal J (2013) Selective conversion of CO₂ to CO with high efficiency using an inexpensive bismuth-based electrocatalyst. *J Am Chem Soc* 135:8798–8801. <https://doi.org/10.1021/ja4033549>
50. Medina-Ramos J, Pupillo RC, Keane TP, Di Meglio JL, Rosenthal J (2015) Efficient conversion of CO₂ to CO using tin and other inexpensive and easily prepared post-transition metal catalysts. *J Am Chem Soc* 137:5021–5027. <https://doi.org/10.1021/ja5121088>
51. Alvarez-Guerra M, Albo J, Alvarez-Guerra E, Irabien A (2015) Ionic liquids in the electrochemical valorisation of CO₂. *Energy Environ Sci* 8:2574–2599. <https://doi.org/10.1039/C5EE01486G>
52. Hiejima KH, Hayashi Y, Uda M, Oya A, Senboku SK, Takahashi H (2010) Electrochemical carboxylation of *a*-chloroethylbenzene in ionic liquids compressed with carbon dioxide. *Phys Chem Chem Phys* 12(12):1953–1957
53. Chen Y, Mu T (2019) Conversion of CO₂ to value-added products mediated by ionic liquids. *Green Chem* 21:2544–2574. <https://doi.org/10.1039/B920413J>
54. Pardal T, Messias S, Sousa M, Machado ASR, Rangel CM, Nunes da Ponte M, Pinto JV, Martins R, Nunes da Ponte M (2017) Syngas production by electrochemical CO₂ reduction in an ionic liquid based-electrolyte. *J CO₂ Util* 18:62–72. <https://doi.org/10.1016/j.jcou.2017.01.007>
55. Messias S, Sousa MM, Nunes da Ponte M, Rangel CM, Pardal T, Machado ASR (2019) Electrochemical production of syngas from CO₂ at pressures up to 30 bar in electrolytes containing ionic liquid. *React Chem Eng* 4:1982. <https://doi.org/10.1039/C9RE00271E>
56. Mizuno T, Ohta K, Sasaki A et al (1995) Effect of temperature on electrochemical reduction of high-pressure CO₂ with In, Sn, and Pb electrodes. *Energy Sources* 17:503–508. <https://doi.org/10.1080/00908312>
57. Ramdin M, Morrison ART, De Groen M et al (2019) High-pressure electrochemical reduction of formic acid/formate: effect of pH on the downstream separation process and economics. *Ind Eng Chem Res* 58:22718–22740. <https://doi.org/10.1021/acs.iecr.9b03970>
58. Morrison ART, van Beusekom V, Ramdin M et al (2019) Modeling the electrochemical conversion of carbon dioxide to formic acid or formate at elevated pressures. *J Electrochem Soc* 166:E77–E86. <https://doi.org/10.1149/2.0121904jes>
59. Sabatino S, Galia A, Saracco G, Scialdone O (2017) Development of an electrochemical process for the simultaneous treatment of wastewater and the conversion of carbon dioxide to higher value products. *ChemElectroChem* 4:150–159. <https://doi.org/10.1002/celec.201600475>
60. Jhong HRM, Brushett FR, Kenis PJA (2013) The effects of catalyst layer deposition methodology on electrode performance. *Adv Energy Mater* 34:589–599. <https://doi.org/10.1002/aenm.201200759>
61. Perry R, Green D (2008) Perry's chemical engineers' handbook
62. Scialdone O, Galia A, Guarisco C et al (2008) Electrochemical incineration of oxalic acid at boron doped diamond anodes: role of operative parameters. *Electrochim Acta* 53:2095–2108. <https://doi.org/10.1016/j.electacta.2007.09.007>
63. Dufek EJ, Lister TE, McIlwain ME (2011) Influence of S contamination on CO₂ reduction at Ag electrodes. *J Electrochem Soc* 158:B1384–B1390. <https://doi.org/10.1149/2.051111jes>
64. Hori Y, Ito H, Okano K et al (2003) Silver-coated ion exchange membrane electrode applied to electrochemical reduction of carbon dioxide. *Electrochim Acta* 48:2651–2657. [https://doi.org/10.1016/S0013-4686\(03\)00311-6](https://doi.org/10.1016/S0013-4686(03)00311-6)
65. Rosen J, Hutchings GS (2016) Mechanistic insights into the electrochemical reduction of CO₂ to CO on nanostructured Ag surfaces. *ACS* 5:4293–4299. <https://doi.org/10.1021/acscatal.5b00840>
66. Sun K, Wu L, Qin W et al (2016) Enhanced electrochemical reduction of CO₂ to CO on Ag electrocatalysts with increased unoccupied density of states. *J Mater Chem A* 4:12616–12623. <https://doi.org/10.1039/c6ta04325a>
67. Hsieh Y-C, Senanayake SD, Zhang Y et al (2015) Effect of chloride anions on the synthesis and enhanced catalytic activity of silver nanocoral electrodes for CO₂ electroreduction. *ACS Catal* 5:5349–5356. <https://doi.org/10.1021/acscatal.5b01235>
68. He Z, Liu T, Tang J et al (2016) Highly active, selective and stable electroreduction of carbon dioxide to carbon monoxide on a silver catalyst with truncated hexagonal bipyramidal shape. *Electrochim Acta* 222:1234–1242. <https://doi.org/10.1016/j.electacta.2016.11.097>
69. Kuhl KP, Hatsukade T, Cave ER et al (2014) Electrocatalytic conversion of carbon dioxide to methane and methanol on transition metal surfaces. *J Am Chem Soc* 136:14107–14113. <https://doi.org/10.1021/ja505791r>
70. König M, Vaes J, Klemm E, Pant D (2019) Solvents and supporting electrolytes in the electrocatalytic reduction of CO₂. *Science* 19:135–160. <https://doi.org/10.1016/j.isci.2019.07.014>
71. Verma S, Lu X, Ma S et al (2016) The effect of electrolyte composition on the electroreduction of CO₂ to CO on Ag based gas diffusion electrodes. *Phys Chem Chem Phys* 18:7075–7084. <https://doi.org/10.1039/C5CP05665A>
72. Jarvis SM, Samsatli S (2018) Technologies and infrastructures underpinning future CO₂ value chains: a comprehensive review and comparative analysis. *Renew Sustain Energy Rev* 85:46–68. <https://doi.org/10.1016/j.rser.2018.01.007>
73. Jouny M, Luc W, Jiao F (2018) General techno-economic analysis of CO₂ electrolysis systems. *Ind Eng Chem Res* 57:2165–2177. <https://doi.org/10.1021/acs.iecr.7b03514>
74. Spurgeon JM, Kumar B (2018) A comparative techno-economic analysis of pathways for commercial electrochemical CO₂ reduction to liquid products. *Energy Environ Sci* 11:1536–1551. <https://doi.org/10.1039/c8ee00097b>
75. Rumayor M, Perez P, Irabien A (2019) A techno-economic evaluation approach to the electrochemical reduction of CO₂ for formic acid manufacture. *J CO₂ Util* 34:490–499. <https://doi.org/10.1016/j.jcou.2019.07.024>

Publisher's Note Springer Nature remains neutral with regard to jurisdictional claims in published maps and institutional affiliations.